

## Spin-wave reciprocity in the presence of Néel walls

Körber, L.; Wagner, K.; Kákay, A.; Schultheiß, H.;

Originally published:

October 2017

**IEEE Magnetics Letters 8(2017), 4109804**

DOI: <https://doi.org/10.1109/LMAG.2017.2762642>

Perma-Link to Publication Repository of HZDR:

<https://www.hzdr.de/publications/Publ-26179>

Release of the secondary publication  
on the basis of the German Copyright Law § 38 Section 4.

# Spin-wave reciprocity in the presence of Néel walls

Lukas Körber<sup>1,2</sup>, Kai Wagner<sup>1,2</sup>, Attila Kákay<sup>1</sup>, Helmut Schultheiss<sup>1,2</sup>

<sup>1</sup>*Helmholtz-Zentrum Dresden - Rossendorf, Bautzner Landstrasse 400, 01328, Dresden, Germany,*

<sup>2</sup>*Technische Universität Dresden, D-01062, Dresden, Germany*

**Abstract**—The reciprocity of spin-wave propagation in  $180^\circ$  Néel walls and surrounding domains is studied. For this, the dispersion relation, phase fronts and spin-wave intensities are analyzed via micromagnetic simulations. Despite the in-plane curling of the magnetization, the domain wall itself acts as a reciprocal channel, whereas non-reciprocal spin-wave propagation is found within the domains. Since the spin-wave localization depends on the selected frequency, this may allow to control the degree of propagation asymmetry.

**Index Terms**—Nanomagnetics, domain wall, reciprocity, spin waves

Under certain circumstances spin waves in a ferromagnet show non-reciprocal behavior, which is to say that they change their characteristics upon reversal of their propagation direction. This non-reciprocity can have several different origins. The most known example are the Damon-Eshbach modes in thin-film ferromagnets [1], where the spin-wave localization switches from the top to the bottom surface under inversion of their propagation direction. This effect is emphasized by different anisotropies at the top and bottom surfaces [2]. Moreover, it has been shown that the interfacial Dzyaloshinskii-Moriya Interaction, arising from the broken inversion symmetry of the surfaces, leads to additional asymmetric spin-wave dispersions [3]–[6]. Similar non-reciprocal spin-wave propagation is observed, when the top and bottom layers of a thin-film bi-layer system are of different magnetic material and/or antiferromagnetically coupled [7], [8]. Transitioning from plane to curved surfaces, the magnetostatic and exchange interactions are modified [9], [10] and result, for instance, in an asymmetric dispersion relation in magnetic tubes, as recently shown in [11].

In all of these cases, the non-reciprocal spin-wave propagation arises from the interplay of two (curved) surfaces or layers.

However, the strong dependence of the spin-wave dispersion on the angle between the wave vector and the magnetization [12] raises the question whether non-reciprocity can also arise solely from a curvature of the equilibrium magnetization such as the curling in domain walls. In Néel type domain walls the magnetization continuously rotates on a nanometer-scale between two domains of different orientation. In these domain walls the effective magnetic field is lower with respect to the surrounding domains forming a potential well in which low frequency spin waves can be guided while staying confined to the domain wall [5], [13]. In this letter, the influence of the curling magnetization on the spin-wave dispersion relation, phase fronts and intensities of spin waves in the presence of such domain walls is studied.

For this, micromagnetic simulations using *MuMax*<sup>3</sup> are performed [14]. A rectangular permalloy thin-film stripe of  $10\ \mu\text{m}$  length,  $2\ \mu\text{m}$  width and  $15\ \text{nm}$  thickness is modelled on a  $2048 \times 512 \times 1$  grid with a Gilbert damping of  $\alpha = 0.012$ , a saturation magnetization of  $M_S = 830 \times 10^3\ \text{A/m}$  as well as an exchange-stiffness constant of  $A_{\text{ex}} = 13 \times 10^{-12}\ \text{J/m}$ . To model a quasi-infinite stripe the structure is virtually repeated along its length ( $x$ -direction) by using periodic boundary conditions provided by *MuMax*<sup>3</sup>. As an initial configuration two domains of opposite magnetization are chosen and subsequently relaxed into the ground state. Thereby, a  $180^\circ$  Néel wall is formed parallel to the long axis of the stripe (as shown in Fig. 1 a)). Across the domain wall running along the stripe center the magnetization rotates continuously from the  $+x$  to the  $-x$  direction. Using the definition given by Lilley [15] the width of the Néel wall is estimated to be around  $80\ \text{nm}$ .

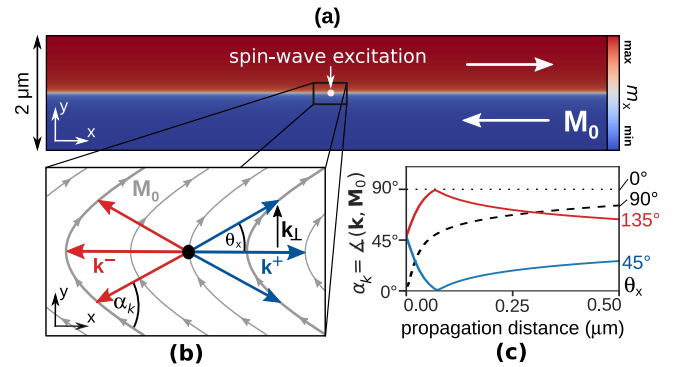


Figure 1. **a)** Magnetic configuration of the quasi-infinite  $2\ \mu\text{m}$ -wide permalloy stripe with a  $180^\circ$  Néel wall. White arrows indicate the direction of the oppositely magnetized domains. The color-code indicates the  $x$ -component of the magnetization. **b)** The continuous curling of the magnetization (gray lines) is schematically shown for a smaller region at the domain wall. When exciting dynamics at a point-like region (black dot) spin waves are radially emitted in directions defined by the propagation-angle  $\theta_x$  with respect to the  $x$ -axis. The angle enclosed by the wave vector and the curling magnetization is locally defined by  $\alpha_k$ . **c)** For the Néel wall configuration, different propagation characteristics, influenced by  $\alpha_k$ , are expected under mirror-inversion of  $\theta_x$ , as shown for the case of wave vectors along  $90^\circ$ ,  $45^\circ$  and  $135^\circ$ .

Spin waves are excited at a point-like region by applying a time dependent external field at the center of the  $180^\circ$  Néel wall in the ferromagnetic stripe. In order to reduce reflections, a gradually increasing damping profile is introduced within a  $300\ \text{nm}$  wide shell at the stripe edges as an absorbing boundary layer. The emitted spin-waves can be described by their wave vector contribution defining their propagation direction in space  $\theta_x$  and angle with respect to the underlying magnetic configuration  $\alpha_k = \angle(\mathbf{k}, \mathbf{M}_0)$ . Spin waves travelling towards the

$x$ -direction consist of equal wave vector magnitude pointing towards  $\pm\theta_x$ , due to their opposite transversal  $k_\perp$  but equal wave vector along the wall  $k_\parallel$ , exhibiting a small spin-wave amplitude within the domains. In Fig. 1 **b**) these wave vectors associated with the opposite propagation directions  $\mathbf{k}^+$  and  $\mathbf{k}^-$  (including the transversal component  $k_\perp$ ) are schematically shown together with the curling magnetization at the domain wall. The local rotation of the magnetization introduces an asymmetry: Spin waves associated with  $\mathbf{k}^+$  will experience a different range of angles  $\alpha_k$  between their wave vectors and the magnetization than those associated with  $\mathbf{k}^-$ . Due to the anisotropic thin-film dispersion of spin waves an influence on the spin-wave propagation characteristics is expected. Fig. 1 **c**) shows the locally varying angle  $\alpha_k = \angle(\mathbf{k}, \mathbf{M}_0)$  along opposite propagation directions ( $\theta_x^+ = 45^\circ$  and  $\theta_x^- = 135^\circ$ ) as well as  $\theta_x = 90^\circ$ . As an example for the (+)-direction, an angle to the domain wall of  $\theta_x = 45^\circ$  will result in a wave vector which is rather parallel to the magnetization ( $\alpha_k < 45^\circ$ ). In contrast to this, under inversion of propagation to the (-)-direction ( $\theta_x = 135^\circ$ ) the wave vector will rather be perpendicular to the magnetization ( $\alpha > 45^\circ$ ). Therefore, it can be assumed that the spin waves associated with  $\mathbf{k}^-$  are more in the Damon-Eshbach regime as opposed to the backward-volume regime associated with  $\mathbf{k}^+$ .

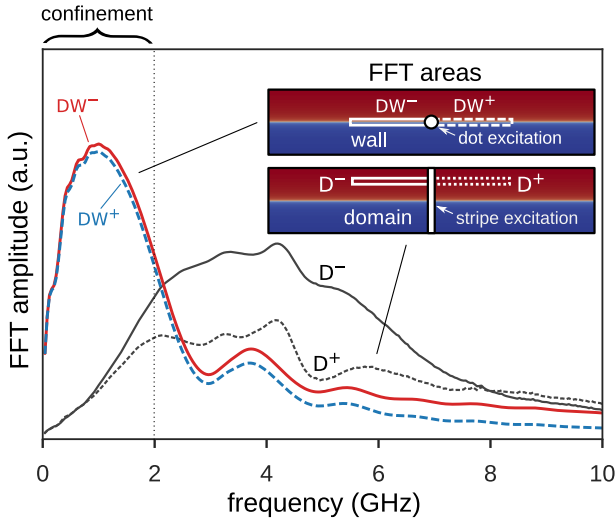


Figure 2. Spatial dependent power spectrum of the magnetization dynamics for the domains and domain wall in opposite propagation directions. The areas of separate spectral analysis are schematically shown in the inset. Confined spin waves with frequencies below 2 GHz contribute predominantly to the domain wall spectra, while the higher frequency spin waves are mainly situated in the domains. In this regime above 2 GHz, the power spectra calculated for the  $D^+$  and  $D^-$  domain areas show an intensity-asymmetry.

To model the point-source and obtain the spin-wave spectrum within the domain wall an out-of-plane field with a gaussian spatial profile ( $\sigma = 50$  nm) and a time dependence of  $\text{sinc}(2\pi f(t - t_0))$  is applied at the center of the stripe to excite modes up to 40 GHz. The resulting time dependent magnetization is fast Fourier transformed at each cell in two different regions with an area of  $5 \mu\text{m} \times 50$  nm to separately examine the spin wave spectra inside the domain wall. The regions are marked as  $DW^-$  and  $DW^+$ . Additionally, to calculate the

spectra in the domains, the excitation is extended to cover the entire width of the stripe so that a homogeneous field pulse across the stripe is achieved. Accordingly, the regions of interest are shifted to the domains and are marked as  $D^-$  and  $D^+$ . Both excitation geometries and the four FFT regions are schematically shown in the inset of Fig. 2.

The resulting spectra shown in Fig. 2 clearly indicate that a confinement of spin waves within the domain wall can be observed at frequencies below 2 GHz, where the spin-wave intensities inside the wall are much higher than in the surrounding domains. Above this frequency, the amplitudes of the spin waves in the domains are more dominant. The spectra calculated for the regions  $DW^-$  and  $DW^+$  within the domain wall are nearly identical. In contrast to this, the spectra within the regions  $D^-$  and  $D^+$  in the domains show significant differences. Hence, non-reciprocal propagation might be assumed, which will be discussed later.

Simulations with continuous wave excitation using a har-

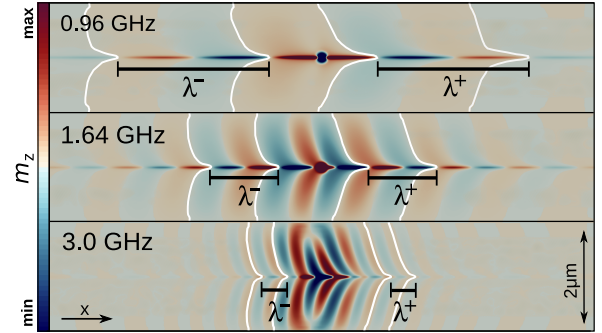


Figure 3. Simulated spin-wave mode-profiles for a continuous wave excitation with a point-source at the center of the domain wall. Snapshots of the out-of-plane component (color-coded) are shown exemplarily for three frequencies. With increasing frequency (top to bottom), the wave-vector magnitude along the domain wall increases, while simultaneously the spin-wave intensities become more pronounced in the domains. Additionally, for each frequency two consecutive phase-fronts for the (+) and (-) propagation directions are highlighted (white lines). The wavelength given by their distance is identical for the oppositely travelling waves within the domain wall, while noticeable differences in the shape of the phase fronts are observed in the domains.

monic time dependence  $B_{\text{ext}} \propto \sin(2\pi ft)$  applied using the point-source in the out-of-plane direction are performed to obtain a closer look at the spin-wave propagation between 0.1 GHz and 6 GHz. In order to rule out numerical errors resulting from using only one cell in  $z$ -direction, equivalent simulations are done with a stripe of 25 nm thickness and an increased number of 5 cells in  $z$ -direction yielding identical results. Snapshots of the spin-wave profiles are shown for three exemplary frequencies in Fig. 3. In agreement with the previously derived spectra, in Fig. 2, spin waves of frequencies below 2 GHz are mostly confined to the domain wall. With increasing frequencies, the magnitude of the wave vector increases, while simultaneously the main spin-wave intensities become more pronounced and finally dominant in the domains. As an example, in Fig. 3 the snapshot at 1.64 GHz already shows a spin-wave radiation into the domains. For better visibility two consecutive phase-fronts both for the (+) and (-) propagation directions are highlighted. The wavelength given

by their distance, shows no difference within the domain wall for the oppositely travelling waves. However, in the domains noticeable changes in the shape of the phase-fronts are observed. Using the phase profiles  $\phi^\pm(x)$  in the domain wall

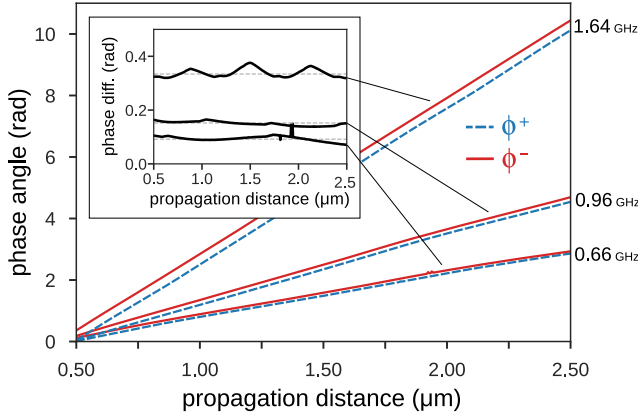


Figure 4. Spin-wave phase profiles  $\phi(x)$  along the domain wall for  $DW^-$  (solid lines) and  $DW^+$  (dashed lines) for three distinct frequencies. Albeit an absolute and constant phase difference (shown in the inset)<sup>1</sup>, the spatial change in phase (slope of each profile) giving the wave-vector magnitude  $k$  along the domain wall is identical for the (-) and (+) propagation directions.

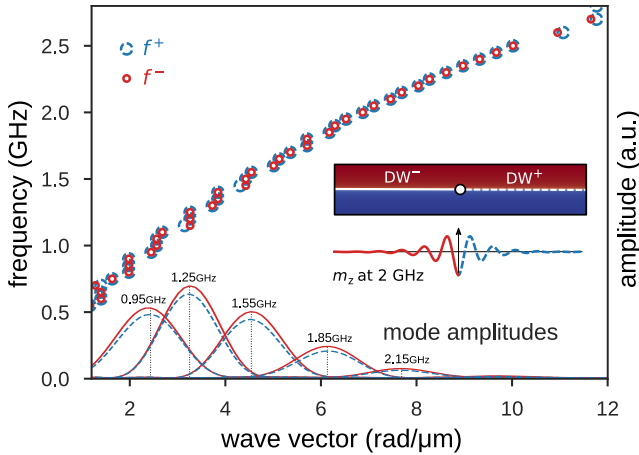


Figure 5. Spin-wave dispersion relation in the domain wall for  $DW^-$  and  $DW^+$  regions, determined from the mode-profile (inset) using continuous wave excitation. The two dispersions are identical within the uncertainty of the spatial Fourier analysis. Additionally, the mode amplitudes along the domain wall are shown for five distinct frequencies. The dispersion was calculated up to spin-wave frequencies of 2.5 GHz, where the spin-wave intensity inside of the domain wall becomes negligible compared to the one in the domains.

and the wave vectors, extracted from Fourier analysis of line profiles, the dispersion relation for both (+) and (-) directions along the domain wall is calculated. This corresponds to the regions marked as  $DW^-$  and  $DW^+$  in Fig. 2. The phase profiles  $\phi^\pm(x)$  along the opposite propagation directions are acquired by calculating the precession ellipse in the coordinate system of the local effective field which corresponds to the local

<sup>1</sup>The oscillations in the phase difference (inset of Fig. 4) are introduced by small numerical inaccuracies related to the ellipticity of the magnetization trajectory.

equilibrium direction of the magnetization  $\mathbf{M}_0$  [16]. The wave-vector magnitude  $k$  along the domain wall is then equivalent to the derivative  $\partial_x \phi$  of the respective phase profile [17].

As seen in Fig. 4 the phase profiles for  $DW^-$  and  $DW^+$ , albeit having an absolute phase difference which increases with the excitation frequency, have an identical slope and therefore equal magnitude of the wave vector. The wave vectors are additionally determined from the out-of-plane component  $m_z$  along the domain wall by spatial Fourier Transformation for a given point in time. The resulting dispersion relation for the domain wall on both sides  $DW^-$  and  $DW^+$  is summarized in Fig. 5 together with the spatial Fourier amplitudes along the domain wall for five distinct frequencies. The wave vectors are determined by extracting the maximum position of the mode amplitudes for all excitation frequencies. The dispersion is calculated up to spin-wave frequencies of 2.5 GHz, where the spin-wave intensity inside the domain wall becomes negligible compared to the one in the domains. This is in agreement with the previous analysis on the spin-wave spectra (Fig. 2) and mode profiles (Fig. 3). Below 0.5 GHz the wave-vector magnitudes are below  $1.2 \text{ rad}/\mu\text{m}$  corresponding to wave lengths above  $5 \mu\text{m}$  and exceed the length of the linescan. While the wave vectors determined from the maximum of the spatial Fourier analysis are identical within the uncertainty of this method, the magnitude of the amplitudes differ on both sides. Despite the pure out-of-plane field excitation geometry, this observation is similar to the asymmetric excitation efficiencies, known from microstrip antennae [18], [19]. Other than that, the dispersion relations for  $DW^-$  and  $DW^+$  including the frequency spectra (Fig. 2) are identical for both sides.

In summary, the reciprocity of spin-wave propagation in  $180^\circ$  Néel walls and surrounding domains is studied. The in-plane curling of the magnetization results in asymmetric spin-wave intensities and phase fronts. This effect is most pronounced for spin waves with their predominant intensities in the domains for frequencies above 2 GHz. However, spin waves below 2 GHz are localized to the domain wall and have only minor intensity in the surrounding domains. Intriguingly for these type of spin waves a symmetric dispersion relation and almost equal intensities for both propagation directions are observed within the domain wall. Hence, we conclude that the curling of the magnetization induces a non-reciprocity of spin-wave propagation in the domains, whereas the domain wall itself acts as a reciprocal channel. This may allow to control the degree of propagation-asymmetry by adjusting the spin-wave frequencies.

#### ACKNOWLEDGEMENTS

We acknowledge financial support from the Deutsche Forschungsgemeinschaft within programme Grant No. SCHU 2922/1-1. The authors also acknowledge Tobias Schneider for computational support.

#### REFERENCES

- [1] R. W. Damon and J. R. Eshbach, "Magnetostatic modes of a ferromagnet slab," *Journal of Physics and Chemistry of Solids*, vol. 19, no. 3-4, pp. 308-320, May 1961.

- [2] O. Gladii, M. Haidar, Y. Henry, M. Kostylev, and M. Bailleul, "Frequency nonreciprocity of surface spin wave in permalloy thin films," *Phys. Rev. B*, vol. 93, p. 054430, Feb 2016. [Online]. Available: <https://link.aps.org/doi/10.1103/PhysRevB.93.054430>
- [3] K. Zakeri, Y. Zhang, J. Prokop, T.-H. Chuang, N. Sakr, W. X. Tang, and J. Kirschner, "Asymmetric spin-wave dispersion on fe(110): Evidence of the dzyaloshinskii-moriya interaction," *Phys. Rev. Lett.*, vol. 104, p. 137203, Mar 2010. [Online]. Available: <https://link.aps.org/doi/10.1103/PhysRevLett.104.137203>
- [4] D. Cortés-Ortuño and P. Landeros, "Influence of the Dzyaloshinskii-Moriya interaction on the spin-wave spectra of thin films," *Journal of Physics: Condensed Matter*, vol. 25, no. 15, p. 156001, Apr. 2013.
- [5] F. Garcia-Sanchez, P. Borys, R. Soucaille, J.-P. Adam, R. L. Stamps, and J.-V. Kim, "Narrow magnonic waveguides based on domain walls," *Phys. Rev. Lett.*, vol. 114, p. 247206, Jun 2015. [Online]. Available: <https://link.aps.org/doi/10.1103/PhysRevLett.114.247206>
- [6] H. T. Nembach, J. M. Shaw, M. Weiler, E. Jué, and T. J. Silva, "Linear relation between Heisenberg exchange and interfacial Dzyaloshinskii-Moriya interaction in metal films," *Nature Physics*, vol. 11, pp. 825–829, Oct. 2015.
- [7] S. Wintz, V. Tiberkevich, M. Weigand, J. Raabe, J. Lindner, A. Erbe, A. Slavin, and J. Fassbender, "Magnetic vortex cores as tunable spin-wave emitters," *Nature Nanotechnology*, vol. 11, no. 11, pp. 948–953, Nov. 2016.
- [8] Y. Henry, O. Gladii, and M. Bailleul, "Propagating spin-wave normal modes: A dynamic matrix approach using plane-wave demagnetizing tensors," *arXiv:1611.06153*, 2016.
- [9] O. V. Pylypovskiy, V. P. Kravchuk, D. D. Sheka, D. Makarov, O. G. Schmidt, and Y. Gaididei, "Coupling of chiralities in spin and physical spaces: The möbius ring as a case study," *Phys. Rev. Lett.*, vol. 114, p. 197204, May 2015. [Online]. Available: <https://link.aps.org/doi/10.1103/PhysRevLett.114.197204>
- [10] Y. Gaididei, V. P. Kravchuk, and D. D. Sheka, "Curvature effects in thin magnetic shells," *Phys. Rev. Lett.*, vol. 112, p. 257203, Jun 2014. [Online]. Available: <https://link.aps.org/doi/10.1103/PhysRevLett.112.257203>
- [11] J. A. Otálora, M. Yan, H. Schultheiß, R. Hertel, and A. Kákay, "Curvature-Induced Asymmetric Spin-Wave Dispersion," *Physical Review Letters*, vol. 117, no. 22, p. 227203, Nov. 2016.
- [12] B. A. Kalinikos and A. N. Slavin, "Theory of dipole-exchange spin wave spectrum for ferromagnetic films with mixed exchange boundary conditions," *Journal of Physics C: Solid State Physics*, vol. 19, no. 35, pp. 7013–7033, Dec. 1986.
- [13] K. Wagner, H. Schultheiss, A. Kákay, A. Henschke, T. Sebastian, and K. Schultheiss, "Magnetic domain walls as reconfigurable spin-wave nanochannels," *Nature Nanotechnology*, vol. 11, 02 2016.
- [14] A. Vansteenkiste, J. Leliaert, M. Dvornik, M. Helsen, F. Garcia-Sanchez, and B. Van Waeyenberge, "The design and verification of mumax3," *AIP Advances*, vol. 4, no. 10, 2014. [Online]. Available: [http://scitation.aip.org/content/aip/journal/adva/4/10/10.1063/1.4899186;jsessionid=HUHNuPJ\\_XLmP7GYcD\\_9JzZ--x-aip-live-02](http://scitation.aip.org/content/aip/journal/adva/4/10/10.1063/1.4899186;jsessionid=HUHNuPJ_XLmP7GYcD_9JzZ--x-aip-live-02)
- [15] B. Lilley, "LXXI. Energies and widths of domain boundaries in ferromagnetics," *The London, Edinburgh, and Dublin Philosophical Magazine and Journal of Science*, vol. 41, no. 319, pp. 792–813, 1950. [Online]. Available: <http://dx.doi.org/10.1080/14786445008561011>
- [16] L. Körber, "Phasenverschiebung und Transmission von Spinwellen durch magnetische Domänenwände," Bachelor Thesis, TU Dresden.
- [17] K. Vogt, H. Schultheiss, S. J. Hermsdoerfer, P. Pirro, A. A. Serga, and B. Hillebrands, "All-optical detection of phase fronts of propagating spin waves in a Ni81Fe19 microstripe," *Applied Physics Letters*, vol. 95, no. 18, p. 182508, 2009. [Online]. Available: <http://dx.doi.org/10.1063/1.3262348>
- [18] T. Schneider, A. A. Serga, T. Neumann, B. Hillebrands, and M. P. Kostylev, "Phase reciprocity of spin-wave excitation by a microstrip antenna," *Phys. Rev. B*, vol. 77, p. 214411, Jun 2008. [Online]. Available: <https://link.aps.org/doi/10.1103/PhysRevB.77.214411>
- [19] V. E. Demidov, M. P. Kostylev, K. Rott, P. Krzysteczko, G. Reiss, and S. O. Demokritov, "Excitation of microwaveguide modes by a stripe antenna," *Applied Physics Letters*, vol. 95, no. 11, p. 112509, 2009. [Online]. Available: <http://dx.doi.org/10.1063/1.3231875>